Ocean Sci. Discuss., 11, 2391–2422, 2014
www.ocean-sci-discuss.net/11/2391/2014/
doi:10.5194/osd-11-2391-2014

Ocean Science
Discussions
Open Access

Reconstructing bottom water temperatures from measurements of temperature and thermal diffusivity in marine sediments

F. Miesner[1,2], **A. Lechleiter**[1], **and C. Müller**[2]

[1]Zentrum für Technomathematik, University of Bremen, Bremen, Germany
[2]FIELAX Gesellschaft für wissenschaftliche Datenverarbeitung mbH, Bremerhaven, Germany

Received: 20 August 2014 – Accepted: 1 October 2014 – Published: 24 October 2014

Correspondence to: F. Miesner (fmiesner@math.uni-bremen.de)

Published by Copernicus Publications on behalf of the European Geosciences Union.

Abstract

Temperature fields in marine sediments are studied for various purposes. Often, the target of research is the steady state heat flow as a (possible) source of energy but there are also studies attempting to reconstruct bottom water temperature variations to understand more about climate history. The bottom water temperature propagates into the sediment to different depths, depending on the amplitude and period of the deviation. The steady state heat flow can only be determined when the bottom water temperature is constant while the bottom water temperature history can only be reconstructed when the deviation has an amplitude large enough or the measurements are taken in great depths.

In this work, the aim is to reconstruct recent bottom water temperature history such as the last two years. To this end, measurements to depths of up to 6 m shall be adequate and amplitudes smaller than 1 K should be reconstructable.

First, a commonly used forward model is introduced and analyzed: knowing the bottom water temperature deviation in the last years and the thermal properties of the sediments, the forward model gives the sediment temperature field.

Next, an inversion operator and two common inversion schemes are introduced. The analysis of the inversion operator and both algorithms is kept short, but sources for further reading are given. The algorithms are then tested for artificial data with different noise levels and for two example data sets, one from the German North Sea and one from the Davis Strait. Both algorithms show good and stable results for artificial data. The achieved results for measured data have low variances and match to the observed oceanographic settings.

Lastly, the desired and obtained accuracy are discussed. For artificial data, the presented method yields satisfying results. However, for measured data the interpretation of the results is more difficult as the exact form of the bottom water deviation is not known. Nevertheless, the presented inversion method seems rather promising due to its accuracy and stability for artificial data. Continuing to work on the development of

OSD
11, 2391–2422, 2014

more sophisticated models for the bottom water temperature, we hope to cover more different oceanographic settings in the future.

1 Introduction

The depth-dependent temperature in marine sediments is governed by the amount of heat-exchange with the water above and the deeper regions of the earth mantle and is conditioned by the thermal properties of the sediment. When the water temperature is time-independent, a steady state is produced where the vertical heat flow is constant – at least in time scales of decades.

Periodically changing water temperatures propagate into the sediment to different depths. A reliable forward model to describe the sediment temperature in the steady state or with (periodically) changing water temperatures exists (see e.g. Lowrie, 2007) and will be introduced in Sect. 2.

Measured and modeled subsurface temperatures are analyzed for different purposes. Two main fields of investigation are the geothermal heat flow and the reconstruction of the ground surface temperature history (Chouinard et al., 2007). Under circumstances where the surface temperature can be regarded as constant, the measured subsurface temperatures show a linear increase with depth, and with this geothermal gradient the heat production in the lower parts of the earth can be determined. If the heat flow is the aim of the investigation, the steady state is strictly required and any disturbance originating from surface temperature variations is regarded as noise. In the deep sea this is often no problem, as the water column already filters the surface temperature variations and the bottom water temperature is (nearly) homogeneous (Davis et al., 2003). In regions with shallower water or onshore this is a rather big problem and is often only solvable by using temperature measurements from deep boreholes.

Studies on the inversion of the bottom water temperatures, in order to subtract the annual deviation from the measured temperatures to obtain the heat flow, belong to the second topic (e.g. Wang and Beck, 1987; Hamamoto et al., 2005). Here, the surface temperature is modeled as a Fourier series and more than one temperature-depth profile is used. The aim is to obtain mean temperatures over time intervals of several years (Chouinard et al., 2007). Deeper measurements are used to reconstruct older climate history.

This work is located in between these two approaches. We are mainly interested in the surface temperature history, but on smaller time scales. The aim is to estimate the bottom water temperature variations in the last one or two years based on only one single measurement of depth dependent temperature and thermal diffusivity. As only one measurement would be required, this could help to understand the (temperature) dynamics of water basins where continuous temperature monitoring is hard to realize (e.g. in the Arctic Ocean).

Additionally, it could be possible to subtract the annual deviation from the depth dependent temperature and thus the heat flow could be calculated in regions where the geothermal gradient cannot be obtained directly from the temperature data.

Besides artificial data sets, we will provide results of tests with two measured data sets from the German North Sea and the Davis Strait. The regions where the measurements are taken are quite different and thus show the broad field of usability of the presented method.

2 Forward model setup

For the theoretical framework, we regard the sediment as a horizontally layered half-space, where we have no temperature change in each of the horizontal directions and thus work with the one-dimensional heat equation:

$$\rho C_v \partial_t T(x,t) = \partial_x(\lambda \partial_x T(x,t)) + \partial_x(\mathrm{v}T(x,t)) + H(x,t),$$

where $x \in \Omega \subset \mathbb{R}_{\geq 0}$ corresponds to the depth below the sea floor at $x = 0$, $t > 0$ is the time, v is the vertical movement of material and H an inner source. The sediment

OSD
11, 2391–2422, 2014

density ρ, specific heat capacity C_v and thermal conductivity λ are typically depth-dependent. In the considered areas, the volumetric heat capacity ρC_v shows only very small changes with depth and will therefore be regarded as constant (see also Clauser, 2006). With the relation $\kappa = \frac{\lambda}{\rho C_v}$ for the thermal diffusivity we can reduce the parameters to only one per layer.

The equation above states that the deviation of the temperature $T(x,t)$ with respect to time equals the amount of diffusion (first term on the right hand side of the equation) plus the heat transported with the material by $\boldsymbol{v}$ (second term) and the generated heat $H(x,t)$. In the settings we model in this work, the advection term $\partial_x(\boldsymbol{v}T(x,t))$ is neglected, as the pore volume is assumed to be rather small and thus fluid flow is rather low. In regions affected by hydrothermal convection this term can make a big difference but in our case it will be neglected.

When using the homogeneous half-space setting, we model the earth's heat source as a steady state heat flow and thus we have no source term. With this reductions we can simplify the heat equation to our model equation

$$\partial_t T(x,t) - \partial_x(\kappa(x)\partial_x T(x,t)) = 0 \quad \forall x > 0, t > 0. \tag{1}$$

2.1 Thermal properties and boundary conditions

The geothermal gradient is the first derivative of the steady state solution with constant homogeneous boundary value at $x = 0$ of this equation: $\partial_x T_{\text{steady}}(x,t) = \frac{q}{\lambda} = g$ for all $x > 0, t > 0$, where we denote the steady state heat flow with q. Here, the bottom water temperature is constant but in the more general case the surface temperature is time-dependent and its deviation propagates into the sediment.

This deviation of the bottom water temperature will be denoted by $T^f_{\text{water}} : \mathbb{R}_{\geq 0} \longrightarrow \mathbb{R}$, where f is a vector of parameters. The parameters in f are to be reconstructed.

With initial and boundary conditions, the model Eq. (1) becomes a solvable initial-boundary-value problem. In geophysical models aiming for temperature fields in the earth, it is quite common to model the region Ω with infinite depth (Jaupart and

OSD
11, 2391–2422, 2014
Water temperatures from marine sediment temperatures
F. Miesner et al.

Mareschal, 2011). In this paper, we will use this approach, however, in the numerical implementation the region will always have a finite depth x_E which is sufficiently large.

The boundary conditions need to be set up to satisfy the physical conditions, which are the stimulation from a one-year-periodic function of the bottom water temperature and a zero-flow-condition at the lower boundary. The geothermal gradient as the solution to the static heat equation will be added after the modeling process. Thus, we can set a homogeneous Neumann condition at the lower boundary in the time dependent part and the Robin boundary condition at the sediment-water-interface. The latter describes the fact, that the heat flows out of the sediment while the sediment is warmer than the water above, and into the sediment while it is cooler.

Knowing the thermal properties of the sediment and the seasonal forcing of the bottom water temperature, we get a full set of equations to determine the temperature in marine sediment at every place and time:

$$\partial_t u(x,t) - \partial_x(\kappa(x)\partial_x u(x,t)) = 0 \qquad \forall x \in \Omega, t > 0 \tag{2}$$

$$\partial_x u(0,t) = h \cdot \left(u(0,t) - T^f_{\text{water}}(t)\right) \qquad \forall t > 0 \tag{3}$$

$$\partial_x u(x_E,t) = 0 \qquad \forall t > 0 \text{ if } x_E < \infty$$

$$\lim_{x\to\infty} \partial_x T(x,t) = 0 \qquad \forall t > 0 \text{ if } x_E = \infty \tag{4}$$

$$u(x,0) = u_0(x) \qquad \forall x \in \Omega. \tag{5}$$

If the thermal diffusivity $\kappa(x)$, the parameters $f \in \mathcal{D}_T$ in a continuous function $T^f_{\text{water}}(t)$ and $g,h \in \mathbb{R}$ are known, a solution to the boundary value problem Eqs. (2)–(5) yields the sediments' temperature $T_{\text{total}}(x,t) = u(x,t)+gx$. Here, $h(t)$ is the heat transfer coefficient and a measure on how well the heat energy passes the sediment–water interface. Brakelmann and Stammen (2006) discuss the value of this coefficient and propose to use an average value of $h = 150\,\text{W}\,\text{m}^{-2}$ for the German North and Baltic Sea.

Discussion Paper | Discussion Paper | Discussion Paper | Discussion Paper |

OSD

11, 2391–2422, 2014

Water temperatures from marine sediment temperatures

F. Miesner et al.

2.2 Bottom water temperature functions

The temperature at the earth's surface is an overlay of many sinusoidal functions with different periods in terms of Fourier series. As we are interested in the deviation of the bottom water temperature for one year, we use the following simple model with only a one-year-period $\omega = \frac{2\pi}{365}$:

$$T^f_{\text{water}}(t) = A + B\cos(\omega t + \varphi(d)), \quad f = (A, B, d)^T, \tag{6}$$

where A and B in °C denote the average temperature and amplitude respectively. The annual minimum takes place on a day $d > 0$, which leads to a phase delay $\varphi(d) = \omega(\frac{365}{2} - d)$ of the cosine function. Since we want to avoid to consider frozen water we restrict the definition space of T^f_{water} to $\mathcal{D}_T = \mathbb{R}_{\geq 0} \times \mathbb{R}_{\geq 0} \times [0, 365]$.

The example data set from the German North Sea shows influences of smaller periods besides the annual deviation, as the average depth is only 100 m (Rhode et al., 2004). Temperature and salinity of the North Sea are mainly governed by a general cyclonic circulation, which renews the water in the time scale of one year (Rhode et al., 2004). Compared to this input from the Atlantic Ocean, the freshwater input from rivers is small. The central part of the North Sea becomes stratified due to heating in the summer, but gets vertically mixed during winter. At the western and southern coasts, the vertical stratification is prevented by strong tidal currents (for detail on the oceanography of the German North Sea see Rhode et al., 2004). Thus, in the North Sea we can assume the simple model for the bottom water temperature to hold. Still we expect the temperature deviation to be a little bit noisy due to the small depth, and we also expect differences from the parameters in different regions, relating to the tidal currents.

Baffin Bay and Davis Strait are governed by the north going West Greenland Current moving temperate saline Irminger Water from the Atlantic Ocean in the top layers and cold low-saline Polar Water in the bottom layers (Ribergaard, 2008). The data set is located in 1300 m depth where the seasonal influence is mostly damped by the water

OSD
11, 2391–2422, 2014

column and the cold Polar Water is dominant. Thus, we expect the parameters A and specifically B to be near 0 °C.

2.3 General behavior

The general behavior of the forward model is depicted in Fig. 1. We used a parameter set typical for the German North Sea of $f = (10.5, 7, 45)^T$ for the bottom water deviation. Here we see, that the sediment experiences a large temperature range over one year in the upper metres. As the depth increases, the covered temperature range gets smaller.

The attenuation of the amplitude with depth is clearly visible and so is the delay of the temperature. We can observe that the current temperature-depth-profile contains the bottom water temperatures from the last three to four months. Following the orange line indicating the day of the highest bottom water temperature, we can observe a decrease in the sediment temperature with depth. In a depth of 4 m the lowest temperature, as evidence of the last winter, is reached and with further increasing depth the temperatures also increase again. The blue line indicating the day of the coldest bottom water temperature shows a mirror-inverted curve.

3 Data

The temperature reconstructing method (to be described in Sect. 4) was tested for artificial and measured data sets containing about 20 data points in a depth of up to 4 m. The artificial data sets were generated using the forward model and adding some white noise, while the example data sets from the German North Sea and the Davis Strait were measured using the FIELAX VibroHeat and HeatFlow measuring devices, respectively. The locations of the example data sets are shown in Fig. 2.

The principle for the measurements of depth dependent thermal parameters originates from the classical method of determining steady-state heat flow values for the oceanic crust from deep sea sediments. Heat flow values are determined based on

OSD
11, 2391–2422, 2014

Fourier's law of thermal conduction from the steady-state (undisturbed) temperature gradient and thermal conductivities. The design of deep sea Lister-type heat flow probes follows the concept by Hyndman et al. (1979) where a thermistor string parallel to a massive strength member penetrates into the sediment by its own weight. 22 thermistors record the sediment temperature during the whole process. The in-situ temperature is determined from the decay of the frictional heat accompanying the penetration, while the thermal conductivity and diffusivity values are calculated from the temperature decay of an artificial, exactly defined, calibrated heat pulse which heats up the sediment. The in-situ thermal gradient can than be calculated.

This method is normally used in deep sea soft sediments, where the heat flow probe penetrates due to its own weight. Shallow water sediments in the North and Baltic Seas are characterized by more shear resistant sediments as sands, tills, and clays, where this classical method of penetration by gravity alone is not applicable. For this reason, a thermistor string has been combined with a standard VKG vibrocorer (Dillon et al., 2012). The measuring procedure follows the classical way: the system is lowered towards the sediment, penetrates the sediment by vibrocoring, rests in the sediment for in-situ temperature measurement and heat pulse decay recording. With this system, a penetration depth of up to 6 m is possible. The accuracy of the thermistor strings is 2 mK and the resolution is 1 mK.

The processing of the raw data from both measuring devices is handled with the same program. This program determines in-situ temperatures and thermal material properties with an inversion algorithm following Hartman and Villinger (2002). Based on the assumption of the thermal decay around a cylindrical symmetric infinite line source, steady state in-situ temperatures, thermal conductivity and thermal diffusivity are determined in an iterative inversion procedure. From thermal conductivity and diffusivity also the volumetric thermal capacity may be determined by $\rho C_v = \lambda/\kappa$, where ρ is the density of the sediment and C_v the heat capacity.

Figure 3 shows depth dependent properties from a measurement in the North Sea north of Borkum in June 2011. Contrary to the general positive temperature gradient in

OSD
11, 2391–2422, 2014

the earth's crust, a temperature decrease with increasing depth appears, i.e. a negative temperature gradient. This is due to the seasonal variation of bottom water temperature in the North Sea. As the measurement was in June, the influence of the warm summer temperatures is seen in the upper thermistors, the decreasing towards the lower is a relict of low winter temperatures.

For the inversion we had various data sets from the German North and Baltic Sea being measured with the VibroHeat device and data sets from the Davis Strait and the Baffin Bay, which were measured using the classic HeatFlow probe. Excluding some measurements from areas within the Baltic Sea where the bottom water temperature deviation differs too much from our simple model Eq. (6), the obtained results where all in the same range of quality and accuracy. The two data sets presented here are picked for the data quality and not the results.

4 Inverse problem setup

4.1 Discretization of the forward model operator

In the inverse problem, we are seeking to determine the bottom water parameters f from (a priori known) values for the geothermal gradient g and the heat transfer coefficient h for the Robin boundary condition and measurements of the thermal diffusivity $\kappa(\tilde{x})$ and the temperature in the sediment $g^{\varepsilon}(\tilde{x},t^{*})$. Here $\tilde{x} \in \mathbb{R}^{k}$ is the depth vector according to the k sensors of the measuring device and $t^{*} > 0$ a fixed time.

Before introducing our solution method to solve this inverse problem, we need to briefly formalize the forward model. It can be shown that the initial-boundary-problem Eqs. (2)–(5) has a unique solution in the weak sense, see e.g. (Evans, 2010). Thus, we can define the forward operator $F : f \mapsto T(x,t)$ mapping the parameters of the bottom water temperature to the solution of the initial-boundary-problem. For this operator, differentiability with respect to f can be shown if the function for the bottom water temperature deviation T^{f}_{water} is continuously differentiable with respect to the parameter

OSD
11, 2391–2422, 2014

f. The continuous differentiability of the cosine function in Eq. (6) with respect to the three parameters A, B and d is obvious.

When interested in greater time scales it is common to model the earth crust as a homogeneous half space, i.e. Ω has infinite depth and the thermal diffusivity κ is constant over the region. In this case, the solution to the initial-boundary-problem is analytical. Thus, in the numerical calculation of the temperature in the sediment the only occurring errors are rounding errors in the scale of the machine accuracy and no discretization errors. However, as we are modeling the sediment as a layered region with finite depth we have two more sources of error: the discretization error and an error resulting from the finite depth.

The discretization is realized using the method of lines. This method and its convergence properties are broadly analyzed by Hanke-Bourgeois (2009). The mesh size and time steps of the discretization as well as the depth of the lower boundary need to be determined such that the numerical solution is not to far away from the true solution. In other words, we determine a parameter setting such that the relative error between the above mentioned analytical solution and the numerical solution does not exceed the limit of 10^{-3} K. We chose this limit in reference to the accuracy of the data obtained with the FIELAX VibroHeat device.

Having access to a numerical and nonlinear forward model $F : \mathbb{R}^3 \rightarrow \mathbb{R}^k$ mapping the three model parameters A, B and d to the numerically approximated temperature for time $t_* > 0$ at points of the depth vector $\tilde{x} \in \mathbb{R}^k$, we can now discuss the inverse method, which is, roughly speaking, based on the observation that F possesses a gradient $\nabla F \in \mathbb{R}_{k\times 3}$. Let us mention already here that this matrix had maximal rank (= 3) in all our numerical examples.

Since the measured sediment temperature (and also the measured thermal diffusivity) may suffer from measurement errors, we assume that our temperature data is a vector g^ε such that $\|g - g^\varepsilon\| \leq \varepsilon$, where g is the undisturbed data. We assume further that an exact parameter vector f^+ exists such that $F(f^+) = g$ (i.e., our model is valid and represents reality). Our aim is to reconstruct f^+.

OSD
11, 2391–2422, 2014

Our study started considering a non-linear iterative Newton algorithm as a first simple approach, which already provided good results. Therefore, we discuss this approach first. For comparison we furthermore adapted the iterative `REGINN` method, published in Rieder (2003), to our needs.

4.2 The Newton algorithm

Sticking to the notation of Rieder (2003), we consider for the solution of the non-linear equation $F(f) = g^{\varepsilon}$ with disturbed data g^{ε} the ongoing iteration

$$f_{n+1}^{\varepsilon} = f_n^{\varepsilon} + s_n^{\varepsilon}, \quad n \in \mathbb{N}. \tag{7}$$

The iteration step s_n^{ε} is to be determined, so that we – ideally – obtain $f_{n+1}^{\varepsilon} = f^{+}$, the exact solution. Obviously, $s_n^{+} = f^{+} - f_n^{\varepsilon}$ solves this equation. The approach of the Newton algorithm is to determine a good approximation to s_n^{+}.

As F is differentiable with derivative ∇F the following equation holds:

$$\nabla F(f_n^{\varepsilon}) s_n^{+} = g - F\left(f_n^{\varepsilon}\right) - E\left(f^{+}, f_n^{\varepsilon}\right) = b_n.$$

Here, $E(v,w)$ denotes the linearization error. This linearization error, and therefore the right side b_n, is not known but only a disturbed version b_n^{δ}. So we approximate s_n^{+} by solving

$$\nabla F\left(f_n^{\varepsilon}\right) s = b_n^{\delta}. \tag{8}$$

For ill posed problems, solving this linear equation can be quite problematic, but as the derivative has full rank we can simply use Gaussian elimination to determine s_n^{ε}.

Applied to our simple model, the iteration converges to a solution of $F(f) = g^{\varepsilon}$. However, as we are not minimizing for the exact right side $b_n = g - F(f^{+})$ but for a disturbed version, the best result may not be the minimal result. Therefore, we stop the iteration, whenever the reconstructed data is about as near to the noisy data g^{ε}, as the noisy data is away from the exact data. Details on this discrepancy principle can be found, e.g., in (Rieder, 2003).

OSD
11, 2391–2422, 2014

Water temperatures from marine sediment temperatures

F. Miesner et al.

4.3 A regularized inexact Gauss–Newton inverse method

For the inversion of the simple model Eq. (6) for the bottom water temperature deviation the Newton algorithm gave stable results (as we will show in Sect. 5). In our numerical experiments a regularization scheme was never necessary, but it could be of importance if we decide to use a more complex input model for the bottom water temperature. This will not be covered in this work, but will be discussed as a suggestion for further research in the last chapter. One advantage of regularization schemes in general and the `REGINN` algorithm published by Rieder (2003) are their proven convergence properties for noisy data or ill-conditioned non-linear equations.

The `REGINN` algorithm is introduced and analyzed by Rieder (1999a) and Rieder (1999b). The algorithm is an inexact Newton method, i.e. it consists of a outer Newton iteration and an inner regularization iteration, which determines the Newton iteration step. Thus, the outer iteration follows the same idea as the above mentioned simple Newton method Eq. (7), where the iteration step s_n^ε solves Eq. (8), and which is stopped with the discrepancy principle. The determination of the iteration steps can be implemented with any regularization scheme and the analysis is done for a general formulation.

For this work, we adapted the algorithm published by Rieder (2003) where the inner iteration is a Conjugate Gradient (CG) method. As we have two nested iterations, we will refer with n to the outer (Newton) iteration and with m to the inner (CG) iteration.

We consider again the Eq. (8)

$$\nabla F\left(f_n^\varepsilon\right) s = b_n^\delta$$

for the Newton iteration step s_n^ε and tackle this linear system using the CG method.

The CG method is designed to minimize the residuum $\|b_n^\delta - \nabla F(f_n^\varepsilon)s_m\|$ in every iteration step $m = 1, 2, 3, \ldots$ in enlarging subspaces. As the residuum at the end of every iteration step is the minimum in the corresponding subspace, the method is the most efficient method possible. For more information on the CG method see e.g. (Rieder,

OSD
11, 2391–2422, 2014

2003; Hanke-Bourgeois, 2009). The inner iteration is stopped, when the linearized residuum fulfills a certain accuracy estimation (for details on the choice of this estimation see Rieder, 2003). The outer iteration is again stopped with the discrepancy principle. Thus, we can directly compare the reconstructions from the two algorithms.

5 Results

5.1 Artificial data for measured thermal diffusivity

In this section, we analyze the sensitivity of the algorithms in a layered half-space setting. Therefore, we used the measured thermal diffusivity and the depth-vector of the sensors, decided on a day of the year t_* and a random vector of the seasonal forcing parameters and produced disturbed data g^ε. For comparability of the results, we used the same water parameters for all the experiments presented here.

As the derivative is not a square matrix, any theoretical analysis of the convergence behavior of the Newton or `REGINN` algorithm does not apply. To cope with this lack of theoretical information on the general behavior of the introduced inverse problem, we executed the algorithms repeatedly with the same parameters and calculated the variances. Thus, we can give a bound for the emerging reconstruction error in dependence on the noise level in the data. The results are shown in Table 1.

For data with a noise level of 0.1 % (see Table 1) the reconstruction error has the same magnitude for both algorithms. As we chose the initial guess randomly from the definition space and the variances are very small, we can state that both algorithms work stably and that the initial guess has no influence.

We find for a noise level of 1.0 % in the data we can get a maximum reconstruction error of about 8 %, while the mean value of all reconstructions is still close to the exact parameter values with a mean error of only 3 % (see Table 1) with both algorithms. This suggests that the overall result of the inversion can be improved by executing the algorithm several times and using the mean value.

OSD
11, 2391–2422, 2014

The overall mean parameter values $f_{\text{overall}} = (8.2923, 6.1074, 62.6449)^T$ yield a relative reconstruction error of $\approx 1.1\,\%$.

5.2 Artificial data with noisy bottom water temperature

In Sect. 5.1, we regarded artificial data for an undisturbed bottom water temperature function. From the water data available via MARNET (2014) for the German North Sea we can derive that this is very unlikely to be accurate. In this section, we will therefore investigate the influence of noise in the bottom water temperature on the accuracy of the reconstruction.

Differently from the white noise added to the data itself, we here use the smaller periods of the cosine series to approximate the occurring errors as well as possible. Thus, this section will give us an insight in sensitivity of the model with respect to the three main parameters, even if the original forcing was more complicated and the measured data contains errors.

For generating artificial data in this section we changed the seasonal forcing to the first 52 summands of the Fourier series for one-year-periodic functions:

$$T^f_{\text{water}}(t) := A + \sum_{i=1}^{52} B_i \cos(i\varpi t + \varphi(d_i)),$$

$$f = (A, B_1, \ldots, B_{52}, d_1, \ldots, d_{52})^T.$$

This cut-off Fourier series approximates periods from one year to one week.

The results of this experiment are presented in the last section of Table 1. We observe a distinct increase in the reconstruction error for a noise level in the data of 1 % from a mean error of 3 % for a undisturbed bottom water temperature function to a mean error of 7 % here. Although the variances do increase, the mean reconstruction result is still a very good approximation to the exact water parameters. This leads to the conclusion that a single reconstruction may differ in large scales from the exact

OSD
11, 2391–2422, 2014

parameter values, while already 20 repeated executions can markedly decrease the reconstruction error. For both algorithms, we find differences between the average results and the exact parameter values of under 0.1 K in the average temperature and the amplitude and one day in the day of the annual minimum. We can observe that the main uncertainty occurs from the determination of the day of the annual minimum.

From the inversions done here, we can conclude that the three main parameters get reconstructed quite well even if the real bottom water temperature function is more complicated than the simple model in Eq. (6).

5.3 Example: Borkum

While we had data sets from three different locations in the German North and Baltic Sea, we will only present one example in detail. The locations of the measurements and the nearest MARNET stations (see MARNET, 2014) are depicted in Fig. 2. All three data sets are broadly discussed by Müller et al. (2013). The quality of the reconstruction results in terms of variances was the same in all three examples. We choose to present the data set north of the island of Borkum, because of organizational reasons: the distance between the data set location and the nearest MARNET station FINO1 is smaller than with the other examples and the recorded water temperatures showed the smallest differences from the chosen bottom water temperature function Eq. (6). Additionally, we had access to the time series and could analyze the applicability of this model equation.

The results of the inversion are listed in Table 2. In comparison to the parameter vector used in Müller et al. (2013) $\tilde{f}_{\text{Borkum}} = (10.4, 6.9, 41)^T$, the overall mean parameters are almost perfect. We see, that the Newton algorithm provides smaller values than the `REGINN` algorithm, but also with smaller variances in the average temperature and the amplitude. The day of the annual minimum resulting from the Newton algorithm seems very unlikely and also has a larger variance.

Taking the mean values from all reconstructions with both algorithms, the values fit to the educated guess. The variance on the day of the annual minimum is here of course

OSD
11, 2391–2422, 2014

quite large, because it was reconstructed differently by the two algorithms. The value corresponds to a SD of ≈ 15 days.

For the bottom water temperature in this area, we had access to the data of the station FINO1. We inverted the water data with the same algorithm and got the parameter vectors $f_{2010} = (10.0, 7.9, 56)^T$ for the data from 2010 and $f_{2011} = (10.4, 7.1, 55)^T$ for 2011. In this particular case, we see changes in the average temperature and the amplitude of less than 1 K between two years and also the day of the annual minimum stays nearly the same. This leads to the assumption, that the simple model for the bottom water temperature fits the natural conditions in this area quite well.

Comparing these parameter vectors to the ones obtained from the inversion (Table 2), we see that the Newton algorithm provided too small values, while the REGINN algorithm yielded too large values. The overall mean fits best, but the day of the annual minimum was better reconstructed with the REGINN algorithm alone.

In the upper panel of Fig. 4, the FINO1 data from 2010 and 2011 are depicted. Additionally, the cosine functions of the mean inversion results are shown. In the lower panel the measured thermal diffusivity (right) and the measured and modeled temperature-depth-profiles are depicted. We can observe, that the temperature interval resulting from the Newton-results is to small, while the REGINN-result has too high temperatures in the second half of the year. From the three cosine functions, the one resulting from the overall mean fits the recorded temperatures best.

For the temperature-depth-profile on the day of the measurement this does not hold. The model with the over all mean result has too high temperatures. The Newton-result fits the measured temperatures better, but only to a depth of 2 m. The REGINN-results fit here best. The not-so-optimal fit of the overall mean results could be due to the uncertainty of the reconstruction of the day of the annual minimum. Shifting the cosine of the overall mean results about one week (such that $d \approx 48$) the cosine would fit the recorded temperatures at FINO1 better and the temperature-depth-profile would also fit the measurements better.

OSD
11, 2391–2422, 2014

5.4 Example: Greenland

The second example data set was measured on a cruise in 2006 in the waters of the Davis Strait and Baffin Bay west of Greenland, the location is shown in the lower panel of Fig. 2. We chose this data set, recorded in the southern part of the Davis Strait over the other measurements of the cruise as no advective influences occurred.

The measurement is located at the southern ridge of the Davis Strait at the passage to the Labrador Sea. The water has a depth of about 1300 m and thus the bottom water temperature deviation is expected to be rather small.

The reconstruction results are shown in Table 3. We observe that both algorithms reconstruct similar values. As continuous measurements of the bottom water temperature deviation is not easy in these parts of the Arctic Sea there are no measurements to compare these values to. However, the obtained temperature interval seems likely.

In Fig. 5, the cosine functions with the reconstructed bottom water function parameters are depicted (upper panel). In the lower panels the measured thermal diffusivity (right) and sediment temperature (left) as well as the modeled temperature are shown. We can observe a wide range of thermal diffusivity values. The reconstructed bottom water temperature deviations do not differ much, nor do the modelled sediment temperatures. They all fit the measured temperatures quite well. Looking at the low variances (Table 3), this indicates a stable method and high applicability.

6 Discussion

The aim of this work was to provide a method to obtain from one instantaneous measurement of depth dependent sediment temperature and thermal diffusivity the parameters of a function modeling the annual bottom water temperature variation. Assuming a homogeneous half-space, we obtained an analytical and a numerically approximated solution. Before we discuss the obtained reconstruction results, we need to determine how much accuracy is desired in geophysical usage.

OSD
11, 2391–2422, 2014

6.1 Desired accuracy of the reconstructed parameters

In comparison to the measured water temperatures (see MARNET, 2014) it is obvious that the mathematical model Eq. (6) neglects a lot of short periodic noise.

In Sect. 5.3, we showed for the station FINO1 that the average temperature A varied about 0.5 K between the years 2010 and 2011 and the amplitude even about 0.8 K. Similar results can be obtained for other stations. Thus, an accuracy of less than 1 K for the parameters A and B would be small enough and far more than is known now for areas that are difficult to access.

The day of the annual minimum only changed about 1 day at FINO1, but was most difficult to reconstruct in all the experiments seen in Sect. 5. This is clearly due to the fact, that the cosine function has a small first derivative around the extrema. Thus, the function Eq. (6) does not change a lot in the weeks around the annual minimum, e.g. it remains over three weeks in the lowest 1 % of the covered temperature interval.

If we consider the desired accuracy of 1 K we just stated, that means that the function remains even 52 days in the accurate interval. Having possible fields of usage in mind (like the Arctic Ocean) we need to obtain an accuracy level based on the relative error – at least for the two temperature-related parameters: reconstruction of a parameter of the order of 0.1 K with an accuracy of ±1 K is not useful. In the experiments with artificial data sets a relative error of magnitude about or slightly less than the relative data error was achieved. The above stated differences in the recorded bottom water temperature at the station FINO1 yield a relative change of about 5 % in the average temperature and 10 % in the amplitude.

Considering all this, we decided to aim for reconstructing the parameters better than $A \pm 5\,\%$, $B \pm 10\,\%$ and $d \pm 10$ days.

6.2 Achieved accuracy of the reconstructed parameters

For the real data sets, we assumed a noise level of 1 %. While we regarded different noise levels in the experiments with artificial data, only the obtained information on

Discussion Paper | Discussion Paper | Discussion Paper | Discussion Paper |

OSD

11, 2391–2422, 2014

Water temperatures from marine sediment temperatures

F. Miesner et al.

data with 1 % noise is relevant for the applicability on real data. As seen in Table 1, we obtained SDs of $A \pm 0.2$ K, $B \pm 0.5$ K and $d \pm 2.5$ for both algorithms. In relative errors this equals $A \pm 2$ % and $b \pm 8$ %. Thus, we achieved the desired accuracy with only 20 repeated inversions. By taking the overall mean of all reconstructions from both algorithms, we were able to decrease the reconstruction error. Here, the variances and SDs increased, but the obtained result was closer to the exact parameter values.

As we changed the function of the bottom water temperature to a cut-off Fourier-series, the variances increased to $A \pm 0.5$ K, $B \pm 1.5$ K and $d \pm 4.8$ days (see Table 1), or in relative errors $A \pm 6$ % and $B \pm 24$ %. Here, the amplitude was less accurate than desired. Still, the mean of the reconstructed values was accurate within the desired interval.

As the variances were smaller for less noisy data in both experiments, we can conclude that both algorithms yield stable results for data with a noise level ≤ 1 % and for a bottom water temperature function which varies from a plain cosine in magnitude of up to 8 % (see Table 1). For higher noise level in the data or the forcing function the methods still converged, but were not accurate enough.

6.3 Applicability to real data

The experiments with artificial data suggested a stable method, whose accuracy could be increased by executing the algorithms repeatedly and using a mean value of results from both algorithms. The reconstruction error did not increase too much, when we changed the function for the bottom water temperature and still reconstructed the main parameters sufficiently accurately.

Using real data sets, we need to take a closer look at the general form of the bottom water temperature deviation in the regarded area. As mentioned above some areas in the Baltic Sea cannot be modeled with our simple model. The data sets from the North Sea, as the one introduced in Sect. 5.3 in contrary yielded stable results, but with rather large variances. However, the results match with the recorded water temperatures. The differences of the results from the two inversion algorithms to the graphically obtained

OSD
11, 2391–2422, 2014

parameter values (used from Müller et al., 2013) are within the desired error bounds. Here, we saw the greatest differences in the day of the annual minimum, but already discussed that it is not possible to determine it more precisely while A and B are only accurate to 1 K.

Lastly, the results from the inversion of the data set west of Greenland have the smallest variances, proposing reliable values. Other surveys on the temperature (and salinity) of the Baffin Bay and Davis Strait gave similar temperature values (see e.g. Ribergaard, 2008). As there are currently no long-term measurements the results of this method are of scientific value, if one trusts them. It is important to note, that matching with the recorded temperatures is not the same as being exact: the recorded temperatures are also measurements with errors and they were not recorded at exactly the same locations as the data sets were taken.

In conclusion, we propose to use the overall mean values from both algorithms, as we do not know the exact parameters and therefore, can not say which algorithm is more reliable. Before reconstructing data sets, one should carefully consider if the simple model Eq. (6) is applicable for the regarded data set. If it is already known, that the sea is layered and not well mixed or if there are strong currents along the sea floor, this method will not give reasonable results. If one finds unreasonable results, this should be interpreted as a strong hint that the simple model and hence the method are not applicable.

7 Conclusions

The presented method could be of major interest for climate researchers and oceanographers, because it may provide oceanographic information for regions where long-term monitoring is not possible or too expensive. However, before applying the method to other regions, the validity of the simple model for the bottom water temperature needs to be carefully discussed.

OSD
11, 2391–2422, 2014

Therefore, a main topic in further research could be the generalization of the bottom water temperature model. The implementation of the inversion algorithms can be easily adapted to reconstruct the parameter vector of other periodical functions. The Fourier series, introduced in Sect. 5.2, would be a reasonable start. The more coefficients of the Fourier series one wants to reconstruct, the more sensors are needed to get a full-rank derivative. For regions with more noise in the bottom water temperature deviation, such as the Baltic Sea, the smaller periods could possibly generate more realistic data, and thus improve the reconstruction results for such data sets.

A piece-wise constant function as in the large scale climate history reconstruction could also be used. Such a model is then possibly capable of reconstructing a-periodic events in the most recent water temperature changes. This would be of great interest for the Baltic Sea (e.g. to identify inflows from the North Sea over the Danish Straits) or the Arctic Sea (e.g. to indicate cold water discharge due to iceberg calving events).

As mentioned in Sect. 2, determining the steady state heat flow is also a large field of interest. If the reconstruction is stable enough, the calculated seasonal influence could be subtracted and thus the the steady state heat flow could be obtained. For now this is not possible, as the heat flow is a constant input parameter to the forward model. Here, further investigation is needed to implement a method, which is capable of reconstructing the heat flow as well.

Over all it is both desirable to get more data sets to compare results of the inversion technique against measurements as well as to develop models for the bottom water deviation that fit more oceanographic settings. This could further verify our method and the used inversion schemes but also broaden the area of application.

Acknowledgements. This work would not have been possible without the kind permission of NSW (Norddeutsche Seekabelwerke) and GEUS (De Nationale Geologiske Undersøgelser for Danmark og Grønland) to use the data sets measured on cruises with partnership of FIELAX.

OSD

11, 2391–2422, 2014

Water temperatures from marine sediment temperatures

F. Miesner et al.

References

Brakelmann, H. and Stammen, J.: Thermal Analysis of Submarine Cable Routes: LSM or FEM?, IEEE-conference PECon, Putra Jaya, Malaysia, 560–565, 2006. 2396

Bundesamt für Seeschifffahrt und Hydrographie: MARNET-Messnetz, available at: http://www.bsh.de/de/Meeresdaten/Beobachtungen/MARNET-Messnetz/index.jsp (last access: 6 June 2014), 2014. 2405, 2406, 2409

Chouinard, C., Fortier, R., and Mareschal, J.-C.: Recent climate variations in the Subarctic inferred from three borehole temperature profiles in Northern Quebec, Canada, Earth Planet. Sc. Lett., 263, 355–369, 2007. 2393, 2394

Clauser, C.: Geothermal energy, in: Landolt-Börnstein, Group VIII: Advanced Materials and Technologies, vol. 1: Energy Technologies, Subvol. C: Renewable Energies, edited by: Heinloth, K., Springer Verlag, Heidelberg-Berlin, 493–604, 2006. 2395

Davis, E. E., Wang, K., Becker, K., and Yashayaev, I.: Deep-ocean temperature variations and implications for errors in sea floor heat flow determinations, J. Geophys. Res., 108, 2034, doi:10.1029/2001JB001695, 2003. 2393

Dillon, M., Müller, C., and Usbeck, R.: Acquiring thermal conductivity data from shear-resistant sediments, Sea Technol., 53, 57–61, 2012. 2399

Evans, L. C.: Partial Differential Equations, American Mathematical Society, Providence, 663 pp., 2010. 2400

Hamamoto, H., Yamano, M., and Goto, S.: Heat flow measurement in shallow seas through long-term temperature monitoring, Geophys. Res. Lett., 32, L21311, doi:10.1029/2005GL024138, 2005. 2393

Hanke-Bourgeois, M.: Grundlagen der Numerischen Mathematik und des Wissenschaftlichen Rechnens, Vieweg+Teubner, Wiesbaden, 840 pp., 2009. 2401, 2404

Hartmann, A. and Villinger, H.: Inversion of marine heat flow measurements by expansion of the temperature decay function, Geophys. J. Int., 148, 628–636, 2002. 2399

Hyndman, R. D., Davis, E. E., and Wright, J. A.: The measurement of marine geothermal heat flow by a multipenetration probe with digital acoustic telemetry and insitu thermal conductivity, Mar. Geophys. Res., 4, 181–205, 1979. 2399

Jaupart, C. and Mareschal, J.-C.: Heat Generation and Transport in the Earth, Cambridge University Press, New York, 464 pp., 2011. 2395

OSD
11, 2391–2422, 2014

Lowrie, W.: Fundamentals of Geophysics, Cambridge University Press, New York, 381 pp., 2007. 2393

Müller, C, Miesner, F., Usbeck, R., and Schmitz, T.: 2 K-criterion: measuring and modelling temperatures and thermal conductivities/diffusivities in shallow marine sediments, Conference on Maritime Energy 2013, TUHH, Hamburg, 475–490, 2013. 2406, 2411, 2416

Omstedt, A. and Axel, L. B.: Modelling the seasonal, interannual, and long-term variations of salinity and temperature in the Baltic proper, Tellus A, 50, 637–652, 1998.

Rhode, J., Tett, P., and Wulff, F.: The Baltic and North Seas: a regional review of some important physical-chemical-biological interaction processes, in: The Seas, vol. 14, chap. 26, edited by: Robinson, A. R. and Brink, K. H., Harvard University Press, 1029–1071, 2004. 2397

Ribergaard, M. H.: Oceanographic Investigations off West Greenland 2011, Danish Meteorological Institute Centre for Ocean and Ice, Copenhagen, 2011. 2397, 2411

Rieder, A.: On the regularization of nonlinear ill-posed problems via inexact Newton iterations, Inverse Probl., 15, 309–327, 1999a. 2403

Rieder, A.: On convergence rates of inexact Newton regularizations, Numer. Math., 88, 347–365, 1999b. 2403

Rieder, A.: Keine Probleme mit Inversen Problemen: Eine Einführung in stabile Lösungen, Vieweg+Teubner Verlag, Wiesbaden, 2003. 2402, 2403, 2404

Wang, K. and Beck, A. E.: Heat flow measurement in lacrustine or oceanic sediments without recording bottom temperature variations, Geophys. Res., 92, 12837–12845, 1987. 2393

OSD

11, 2391–2422, 2014

Table 1. Statistics for the inversion of artificial data. The uppermost part contains the inversion results for artificial data with 0.1 % white noise added, the middle part artificial data with 1.0 % noise. The lowermost part shows inversion results to artificial data with 0.1 % white noise added after the seasonal forcing already contained noise of about 8 %.

Data	Artificial	0.1 %	noise		
exact parameters	*A*	*B*	*d*		
	8.2	5.9	62		
results Newton	*A*	*B*	*d*	mean error	max error
mean	8.1961	5.8857	61.9709	0.3124 %	0.6483 %
variances	0.0004	0.0025	0.0464		
result REGINN	*A*	*B*	*d*	mean error	max error
mean	8.1978	5.8963	61.9620	0.2096 %	0.5850 %
variances	0.0003	0.0013	0.0318		
Data	Artificial	1.0 %	noise		
exact parameters	*A*	*B*	*d*		
	8.2	5.9	62		
results Newton	*A*	*B*	*d*	mean error	max error
mean	8.2245	5.9563	61.8430	2.8837 %	7.2872 %
variances	0.0474	0.2499	2.8912		
result REGINN	*A*	*B*	*d*	mean error	max error
mean	8.3601	6.2585	63.4468	2.6344 %	5.6842 %
variances	0.0246	0.1344	1.6411		
Data	Artificial	0.1 %	noise	8.0 %	water noise
exact parameters	*A*	*B*	*d*		
	8.2	5.9	62		
results Newton	*A*	*B*	*d*	mean error	max error
mean	8.2504	5.8955	62.8765	6.8582 %	17.5380 %
variances	0.2941	2.2165	22.7159		
result REGINN	*A*	*B*	*d*	mean error	max error
mean	8.2923	5.8878	62.2655	8.6890 %	14.9191 %
variances	0.9917	10.0657	29.5053		

OSD
11, 2391–2422, 2014

Water temperatures from marine sediment temperatures

F. Miesner et al.

Table 2. Results of the inversion of the data set from Borkum. The Newton algorithm gives an unlikely estimate for the day of the annual minimum, but the overall mean parameters fit the guess from Müller et al. (2013) almost perfectly.

Data	Borkum		
results Newton	*A*	*B*	*d*
mean	9.7861	5.6583	26.6172
variances	0.0030	0.0210	2.6269
result REGINN	*A*	*B*	*d*
mean	11.9501	9.1510	55.5305
variances	0.0260	0.0886	1.7055
overall results	*A*	*B*	*d*
mean	10.8681	7.4047	41.0739
variances	1.1999	3.1425	213.7791

OSD
11, 2391–2422, 2014

Table 3. Results of the inversion of the data set west of Greenland. Both Algorithms give similar reconstruction values with small variances.

Data	Greenland		
results Newton	*A*	*B*	*d*
mean	3.1770	0.1583	71.5104
variances	0.0003	0.0001	2.1522
result REGINN	*A*	*B*	*d*
mean	3.1764	0.1600	74.2546
variances	2.6×10^{-6}	3.7×10^{-6}	0.9310
overall results	*A*	*B*	*d*
mean	3.1767	0.1591	72.8825
variances	0.0002	5.8×10^{-5}	3.4286

OSD
11, 2391–2422, 2014

Water temperatures from marine sediment temperatures

F. Miesner et al.

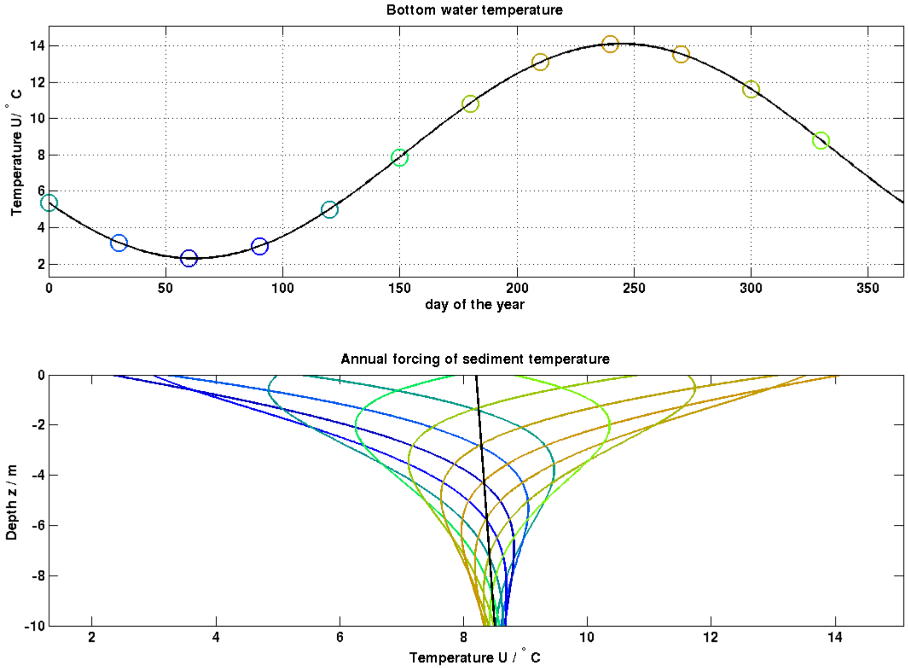

Figure 1. Bottom water temperature (top panel) as input to the forward model operator and the solution (bottom panel) at different days of the year. The bottom water temperature function is a cosine with a mean value of 8.2 °C, an amplitude of ±5.9 K and the minimum on the 62 day of the year. The colors indicate the bottom water temperature and thus the day of the year when the temperature-depth-profile is plotted. The bright orange temperature-depth-profile is the solution on the 220th day of the year, when the bottom water temperature is near the annual maximum of 14.1 °C.

OSD
11, 2391–2422, 2014

Water temperatures from marine sediment temperatures

F. Miesner et al.

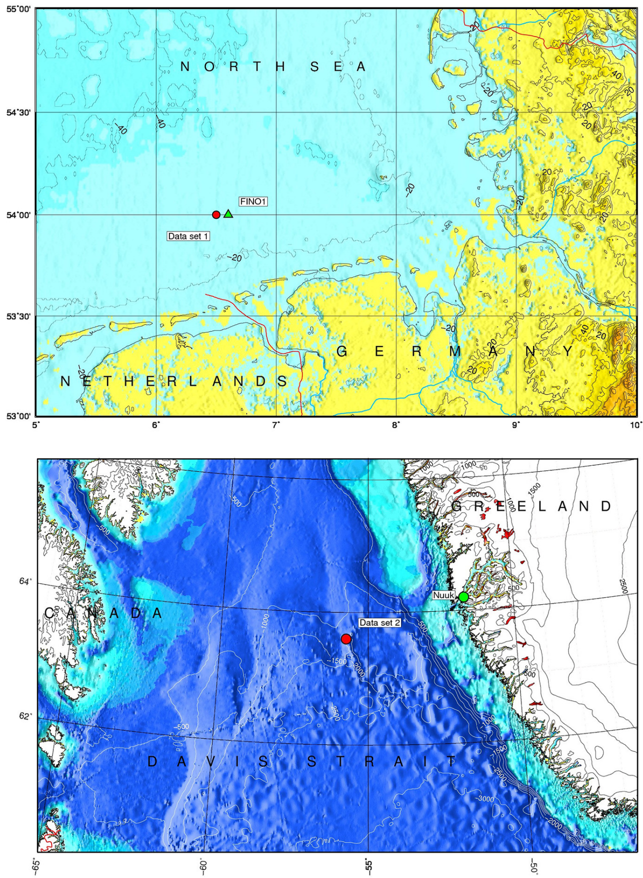

Figure 2. Locations of the two example data sets (red). In the upper panel, the data location near the island of Borkum in the German North Sea is depicted. Additionaly the observation station FINO1 is marked (green). In the lower panel, the data location west of the coast of Greenland near Nuuk is shown.

OSD
11, 2391–2422, 2014

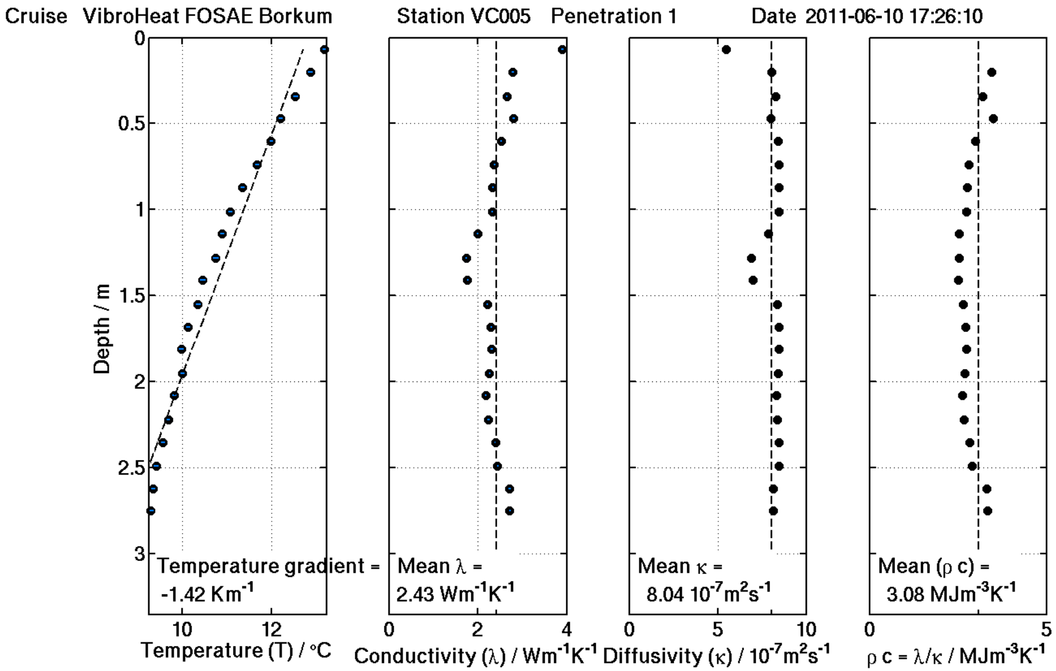

Figure 3. Results of a VibroHeat survey in the North Sea north of Borkum in 2011 showing in-situ temperature, thermal conductivities, thermal diffusivity, and volumetric heat capacity as a function of depth.

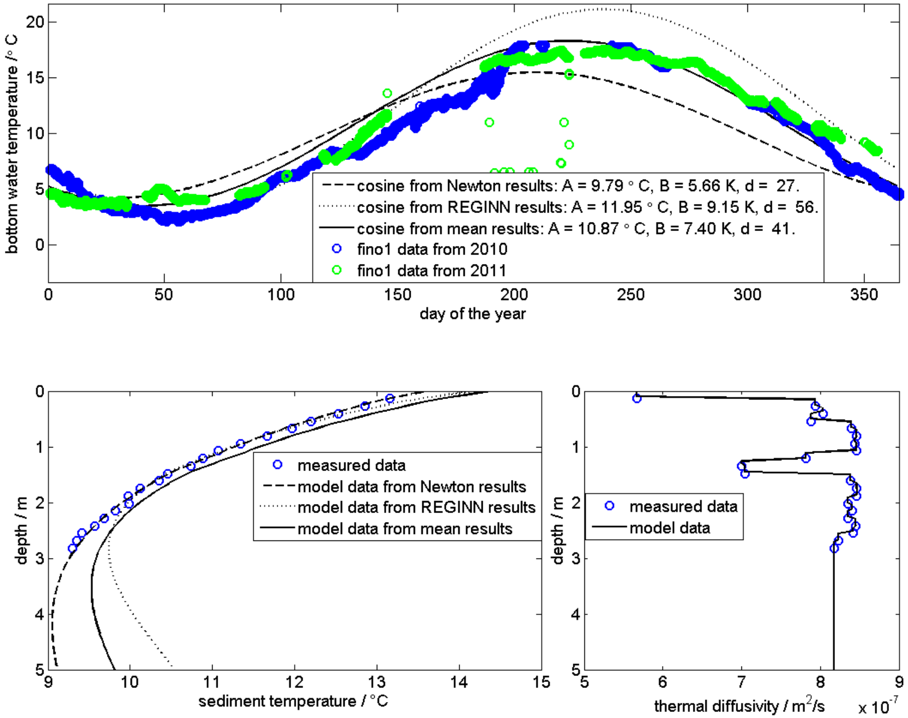

Figure 4. Inversion of the data set near Borkum. In the upper panel, the recorded bottom water temperature at the BSH-station FINO1 are depicted for the years 2010 (green) and 2011 (blue). Additionally, the cosine functions as results of the inversion schemes are plotted: the mean result of the Newton Algorithm, the REGINN result and the overall mean. In the lower panels, the measured temperature (left) and thermal diffusivity (right) are depicted. The resulting temperature-depth-profiles from the modeling with the inversion results are plotted together with the measured temperatures in the left panel.

OSD
11, 2391–2422, 2014

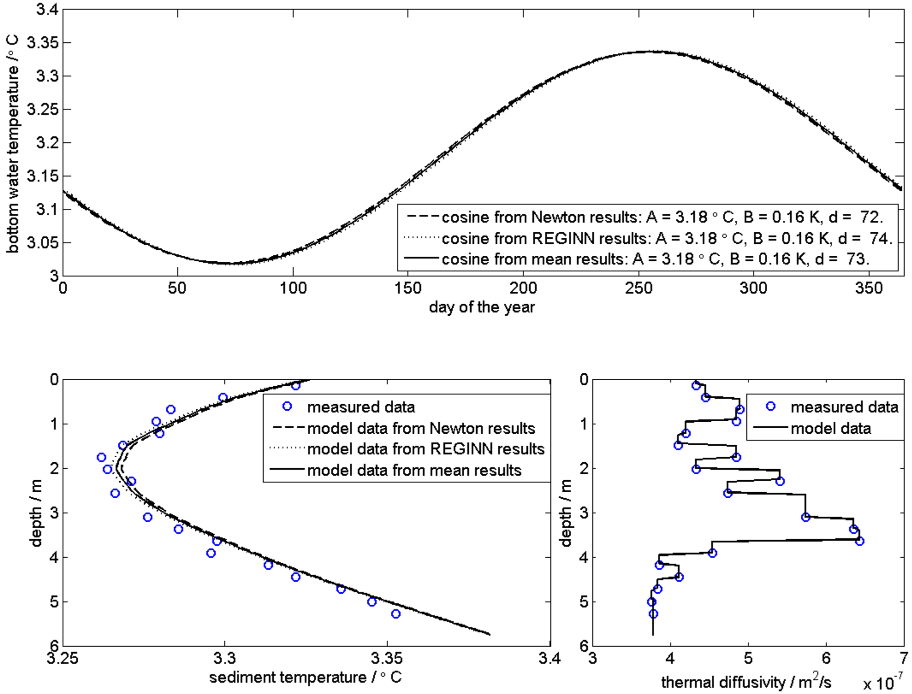

Figure 5. Inversion of the data set west of Nuuk. In the upper panel, the cosine functions as results of the inversion schemes are plotted: the mean result of the Newton Algorithm in dashed line, the REGINN result in dashed line with dots and the overall mean in a straight line. In the lower panels the measured temperature (left) and thermal diffusivity (right) are depicted. The resulting temperature-depth-profiles from the modeling with the inversion results (the line styles are the same as above) are plotted together with the measured temperatures in the left panel.

OSD
11, 2391–2422, 2014

Water temperatures from marine sediment temperatures

F. Miesner et al.